

Experiments on Rayleigh Scattering of 145 keV and 317 keV Photons

S. de Barros, J. Eichler, O. Gonçalves, and M. Gaspar

Instituto de Física, Universidade Federal do Rio de Janeiro, Brasil

Z. Naturforsch. **36a**, 595–599 (1981); received March 23, 1981

Elastic differential cross sections for scattering of photons with 145 keV and 317 keV were measured for Pb, W, Sn, Cd, Ag, Mo and Cu for angles from 5° to 40° . For measuring the strong energy dependence of the cross section at small angles, a well collimated beam ($\pm 0,5^\circ$) and a small detecting solid angle were used. For the energies and angles studied, agreement between experiment and form factor calculations is found. The results are compared with recent measurements of other authors, which found disagreement with form factor calculations.

1. Introduction

Numerous experiments on elastic scattering of photons on atoms in the keV and MeV region have been performed in the last years [1–7]. These investigations are important for cross-section calculations and also because Rayleigh scattering appears as background in x-ray diffraction, nuclear resonance fluorescence and Delbrück scattering. These studies have been stimulated by the development of high resolution Ge(Li) detectors with large volume and by new and more accurate theoretical approaches [8–9, 11–13]. Rayleigh scattering cross-sections are generally calculated using the form factor approximation [8, 9], the modified or anomalous form factor approximation [10, 11] or the second order perturbation theory [12–14].

The form factor theory gives good results for light atoms at energies well above the K-shell binding energy and momentum transfer smaller than $20(\text{\AA})^{-1}$. The modified form factor approximation improves these results for high energies and heavy atoms. The anomalous form-factor approximation can be seriously in error for heavy atoms, if photon energies are greater than several times the K-shell binding energy and if momentum transfer is larger than $10(\text{\AA})^{-1}$. Calculations based in the second order perturbation theory are more accurate. The agreement between these calculations and the existing experimental results is rather good for light and heavy atoms, but shows systematic discrepancy for momentum-transfer in the region $10 - 50(\text{\AA})^{-1}$ [13].

Reprint requests to S. de Barros, Universidade Federal do Rio de Janeiro, Instituto de Física, Cidade Universitária, Ilha do Fundão — Bloco A, 21910 Rio de Janeiro RJ, Brasil.

In the present study we extend some earlier measurements of differential Rayleigh scattering cross sections, where the form factor theory shows deviations from experiment [5, 6], to lower energies and smaller scattering angles. The experiments were performed in the region of momentum transfer $1 - 9 \text{\AA}^{-1}$, where agreement with the form factor approximation is expected [13]. This work was stimulated by the publication of recent measurements in the same momentum transfer region [4, 7], which show discrepancies with the form factor approximation. In the experiments of Ref. [4], NaI detectors were used and the cross sections of Ref. [7] were normalized using Compton cross sections of carbon. It seems desirable to perform similar measurements in which absolute values are obtained using a 0° measurement after reduction of the source activity by natural decay. Therefore, the present measurements, made with a Ge-Li detector, were normalized in this way. The experiment was made for several light, medium and heavy atoms with atomic numbers between 29 and 82 (Cu, Mo, Ag, Cd, Sn, W, Pb) and for photon energies of 145 keV and 317 keV. In Sect. 2 of this work we describe our experimental method and in Sect. 3 results and discussions are presented.

2. Experimental Method

The experiments were carried out using the isotopes ^{192}Ir and ^{141}Ce as sources, with an initial activity of about 50 mCi and with the half lives of 74 days and 32 days, respectively. The Iridium source (60 mg) consisted of a circular metal sheet with a diameter of 4 mm and the Cerium source (2 g) of CeO_2 pressed into a lucite cylinder with

0340-4811 / 81 / 0600-0595 \$ 01.00/0. — Please order a reprint rather than making your own copy.



Dieses Werk wurde im Jahr 2013 vom Verlag Zeitschrift für Naturforschung in Zusammenarbeit mit der Max-Planck-Gesellschaft zur Förderung der Wissenschaften e.V. digitalisiert und unter folgender Lizenz veröffentlicht: Creative Commons Namensnennung-Keine Bearbeitung 3.0 Deutschland Lizenz.

Zum 01.01.2015 ist eine Anpassung der Lizenzbedingungen (Entfall der Creative Commons Lizenzbedingung „Keine Bearbeitung“) beabsichtigt, um eine Nachnutzung auch im Rahmen zukünftiger wissenschaftlicher Nutzungsformen zu ermöglichen.

This work has been digitalized and published in 2013 by Verlag Zeitschrift für Naturforschung in cooperation with the Max Planck Society for the Advancement of Science under a Creative Commons Attribution-NoDerivs 3.0 Germany License.

On 01.01.2015 it is planned to change the License Conditions (the removal of the Creative Commons License condition "no derivative works"). This is to allow reuse in the area of future scientific usage.

an inner diameter of 8 mm. The sources were irradiated in the nuclear research reactor of São Paulo. For ^{141}Ce just one strong line with 145 keV appears while from the numerous lines of ^{192}Ir only the 317 keV line was considered in the experiments. Results for another strong line at 468 keV are reported in a preceeding paper [6]. In Table 1, the targets for the measurements with ^{192}Ir and ^{141}Ce are described. The targets were centered perpendicularly to the incident beam for all scattering angles. In all cases, the product of the attenuation coefficient μ and the target thickness t was in the region $0.4 < \mu t < 1.0$. In this region, double Rayleigh scattering is negligible [7, 15].

For measuring the strong angular dependence of the differential elastic scattering cross section at small angles, the solid angles involved in the experiment must be small. Thus, the targets were placed at distances of 102 cm and 113 cm from the source and the detector, respectively, for scattering angles between 5° and 22° . In order to diminish the solid angle viewed by the detector a 20 mm vertical slit was placed in front of the detector. With the purpose of reducing the background, the incident gamma-beam was collimated within $\pm 0.5^\circ$, yielding an area of constant flux only some millimeters larger than the target. For some measurements (26° , 34° and 40°), where the angular dependence of the cross sections is not too strong and the counting rate is small, the slit in front of the detector was removed. In addition, the distances target-detector and target-source were reduced, reaching minimal values at 40° (51 cm and 36 cm, respectively). The position of the target was controlled by a conventional optical method using a mirror. The scattering angle was measured with an ac-

curacy of approximately 4 minutes using a theodolite centered at the target place. The scattered photons were analyzed with a Ge(Li) detector with a resolution (FWHM) of 4 keV at 1.33 MeV. The detector system was carefully shielded with lead. The spectra of the scattered photons were accumulated with a spectrometric system consisting of pre-amplifier, amplifier and 4 K multichannel analyser. Due to the low counting rate in all cases, measuring times for the scattered spectra between 5 and 30 hours were necessary. The stability of the system was regularly checked using a weak ^{192}Ir or ^{241}Am source. Care has also been taken to minimize the scattering by the target holder, which was therefore made using a small aluminium sheet.

Due to the small solid angles in the experiment, a sharp Compton line just a few keV wide appears and the separation between elastic and inelastic scattering is good. The areas under the elastic peak were fitted with a Gaussian curve.

The background was measured for each scattering angle removing the target from the γ beam. In the background spectrum for the Ir^{192} and Ce^{141} sources no peak at 317 keV or 145 keV was visible.

The differential cross section $d\sigma/d\Omega$ was evaluated using the equation

$$\frac{d\sigma}{d\Omega} = (A_d/\Omega_d) / [(A_s \Omega_t/\Omega_s) N f e^{-T/\tau}]. \quad (1)$$

A_d/Ω_d is the number of the scattered photons per second which are detected divided by the solid angle Ω_d of the detector.

$A_s \Omega_t/\Omega_s$ represents the measured number of photons per second which are incident on the target. This number was determined in a separate experiment, where the source was put at an angle of 0° about 2 m from the detector, yielding the counting rate A_s . The solid angle of the target in this case is Ω_s and the solid angle of the detector as viewed by a point like source is Ω_t . Since the same detector was used in this measurement, the detector efficiency does not enter into the expression for the differential cross section $d\sigma/d\Omega$.

N is the number of the target atoms per cm^2 .

$e^{-T/\tau}$ gives the correction due to radioactive decay of the source where T is the time interval between the scattering experiment and the 0° experiment, and τ is the decay time constant.

f is a correction factor which takes into account the attenuation of the incident and scattered beam.

Element Z	Thickness t (g/cm^2)		
	I	II	III
13	5.28	2.28	5.30
29	5.52	5.52	—
42	5.09	5.09	—
47	4.25	4.25	—
48	5.98	5.98	1.46
50	6.33	7.69	—
74	1.89	1.89	0.494
82	2.52	2.67	0.590

Tab. 1. Targets used for the different experiments.

I: 317 keV, $\theta = 5^\circ - 22^\circ$, dimensions $2 \text{ cm} \times 6 \text{ cm}$.
 II: 317 keV, $\theta = 26^\circ - 40^\circ$, dimensions $4 \text{ cm} \times 10 \text{ cm}$.
 III: 145 keV, $\theta = 15^\circ - 40^\circ$, dimensions $2 \text{ cm} \times 6 \text{ cm}$.

The attenuation factor f is given by

$$f = (1/\cos \theta - 1) \cdot \mu t / [\exp(-\mu t) - \exp(-\mu t/\cos \theta)], \quad (2)$$

where μ is the total gamma ray absorption coefficient in cm^2/g [16, 17], θ is the scattering angle and t the thickness of the target in g/cm^2 . In deriving this equation it was taken into account that the target was always perpendicular to the incident beam and that the thickness of the target is smaller than its width.

The errors in determining the area under the elastic peak due to counting statistics and subtraction of the background are mostly in the region of 1–5%, and only for some cases they reach 10%. The geometrical systematic errors in the solid angles were $\cong 2-4\%$ depending on the geometry used. The precision of the 0° experiment for determining A_s is estimated to be 1%. The correction factor f depends on the total gamma ray absorption coefficient μ (see (2)). In the evaluation of the experimental data given in Tables 2–3 the values μ of Ref. [16] were used. An independent experiment was performed to measure μ , yielding deviations of 1–4%. For 145 keV our values lie between the results of Ref. [16] and some newer measurements [17]. The mean error of f is estimated to be 2%. The errors in the cross-sections given in tables 2–3 are between 7 and 10% for

317 keV and somewhat larger at the other energy studied.

Using the Monte-Carlo-Method, the distribution of the scattering angle due to finite size of source, target and detector, $H(\theta)$, was calculated in steps of 0.2° [18]. The total width of $H(\theta)$ was $\pm 1.5^\circ$ for scattering angles between 5° and 22° . For higher angles the slit in front of the detector was removed and the distance between target and detector was diminished yielding a larger total width of $\pm 3^\circ$. To consider the variation of the cross-section within the distribution $H(\theta)$ a mean weighted angle $\bar{\theta}$ was calculated:

$$\bar{\theta} = \int H(\theta) \frac{d\sigma(\theta)}{d\Omega} \theta d\theta / \int H(\theta) \frac{d\sigma(\theta)}{d\Omega} d\theta. \quad (3)$$

For the differential cross-section $d\sigma/d\Omega$, theoretical values tabulated by Hubbel were used. $\bar{\theta}$ is smaller by about $2'-4'$ than the angle defined by the centers of source, target and detector for angles between $5^\circ-22^\circ$. For higher angles the maximum difference is $7'$. In Tables 2–3 the weighed scattering angle of (3) is given.

3. Results and Discussion

In Tables 2 and 3 we present the measured cross-sections for Rayleigh scattering on Cu, Mo, Ag, Cd, Sn, W and Pb with photon energies of 145 keV and

$\bar{\theta}$	Z	Pb 82	W 74	Cd 48	Δq (\AA^{-1})
$15^\circ \pm 5'$		$28.0 \pm 9\%$	$21.4 \pm 9\%$	$7.2 \pm 11\%$	1.5
$21^\circ 58' \pm 5'$		$13.3 \pm 8\%$	$11.9 \pm 7\%$	$2.65 \pm 8\%$	2.2
$29^\circ 58' \pm 8'$		$7.2 \pm 11\%$	$4.7 \pm 12\%$	$1.52 \pm 10\%$	3.0
$39^\circ 55' \pm 12'$		$2.6 \pm 14\%$	$1.78 \pm 10\%$	$0.73 \pm 14\%$	4.0

Tab. 2. Cross sections for elastic scattering $d\sigma/d\Omega$ (in units of 10^{-24} cm^2) — 145 keV.

Tab. 3. Cross sections for elastic scattering $d\sigma/d\Omega$ (in units of 10^{-24} cm^2) — 317 keV.

$\bar{\theta}$	Z	Pb 82	W 74	Sn 50	Cd 48	Ag 47	Mo 42	Cu 29	Δq (\AA^{-1})
$5^\circ 7' \pm 4'$		$54.0 \pm 10\%$	$39.0 \pm 9\%$	$18.5 \pm 7\%$	$14.9 \pm 10\%$	$14.8 \pm 10\%$	—	—	1.15
$7^\circ 39' \pm 4'$		$25.0 \pm 10\%$	$20.0 \pm 10\%$	$6.6 \pm 10\%$	$5.2 \pm 10\%$	$4.5 \pm 10\%$	$3.5 \pm 10\%$	$1.42 \pm 10\%$	1.72
$9^\circ 34' \pm 4'$		$17.8 \pm 7\%$	$14.0 \pm 7\%$	$4.1 \pm 8\%$	$3.2 \pm 9\%$	$3.0 \pm 9\%$	$2.35 \pm 9\%$	$0.87 \pm 11\%$	2.14
$11^\circ 46' \pm 4'$		$10.5 \pm 7\%$	$7.2 \pm 14\%$	$2.8 \pm 9\%$	$2.1 \pm 10\%$	$1.78 \pm 8\%$	$1.42 \pm 7\%$	$0.37 \pm 16\%$	2.63
$13^\circ 55' \pm 4'$		$8.3 \pm 10\%$	$5.2 \pm 10\%$	$2.0 \pm 8\%$	$1.79 \pm 8\%$	$1.70 \pm 10\%$	—	$0.31 \pm 9\%$	3.10
$17^\circ 54' \pm 4'$		$3.9 \pm 7\%$	$2.9 \pm 7\%$	$1.03 \pm 7\%$	$0.98 \pm 9\%$	$0.84 \pm 7\%$	$0.62 \pm 9\%$	$0.175 \pm 8\%$	3.98
$21^\circ 54' \pm 4'$		$2.2 \pm 10\%$	$1.72 \pm 10\%$	$0.48 \pm 10\%$	$0.48 \pm 10\%$	$0.47 \pm 8\%$	$0.33 \pm 15\%$	$0.123 \pm 10\%$	4.86
$25^\circ 48' \pm 5'$		$1.53 \pm 8\%$	$1.27 \pm 9\%$	$0.31 \pm 8\%$	$0.25 \pm 9\%$	$0.226 \pm 8\%$	$0.160 \pm 8\%$	$0.058 \pm 10\%$	5.75
$34^\circ 13' \pm 8'$		$0.81 \pm 8\%$	$0.57 \pm 8\%$	$0.140 \pm 8\%$	$0.119 \pm 8\%$	$0.109 \pm 9\%$	$0.083 \pm 8\%$	$0.037 \pm 9\%$	7.48
$39^\circ 52' \pm 10'$		$0.54 \pm 9\%$	$0.30 \pm 9\%$	—	—	$0.088 \pm 9\%$	—	—	8.74

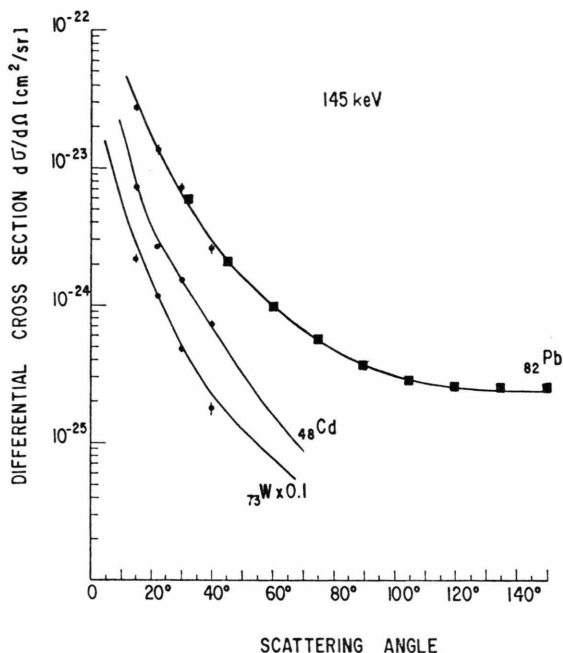


Fig. 1. Experimental results for the 145 keV photon elastic differential cross-sections of Pb, W, Cd compared with (DHFS) calculations (solid lines).

317 keV. The measurements were performed for the angles between 5° and 40° . In Figs. 1 and 2 our experimental results are compared with the cross-sections calculated in the Dirac-Hartree-Fock-Slater (DHFS) form-factor approximation [9]. In Fig. 1,

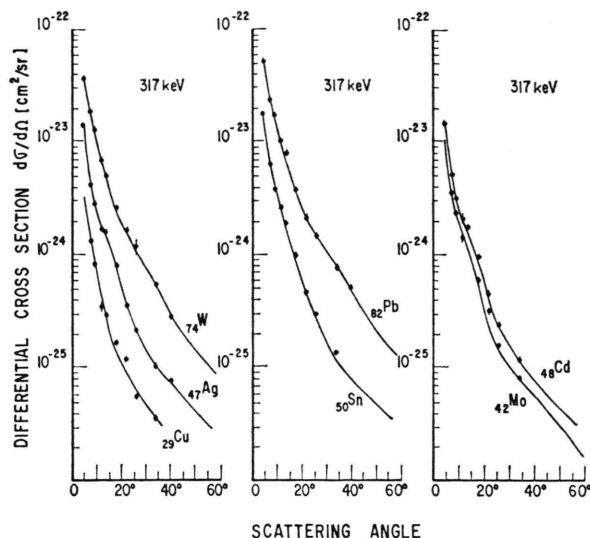


Fig. 2. Experimental results for the 317 keV photon elastic differential cross-sections of Pb, W, Sn, Cd, Ag, Mo, Cu compared with (DHFS) calculations (solid lines).

earlier measurements for higher angles up to 150° are added for Pb [1]. It can be seen that the agreement between the (DHFS) calculations and the experiment is good in all cases studied. We do not find systematic discrepancies between experiment and the form factor theory as stated in Ref. [7] and in Ref. [4] at 145 keV for large atomic number.

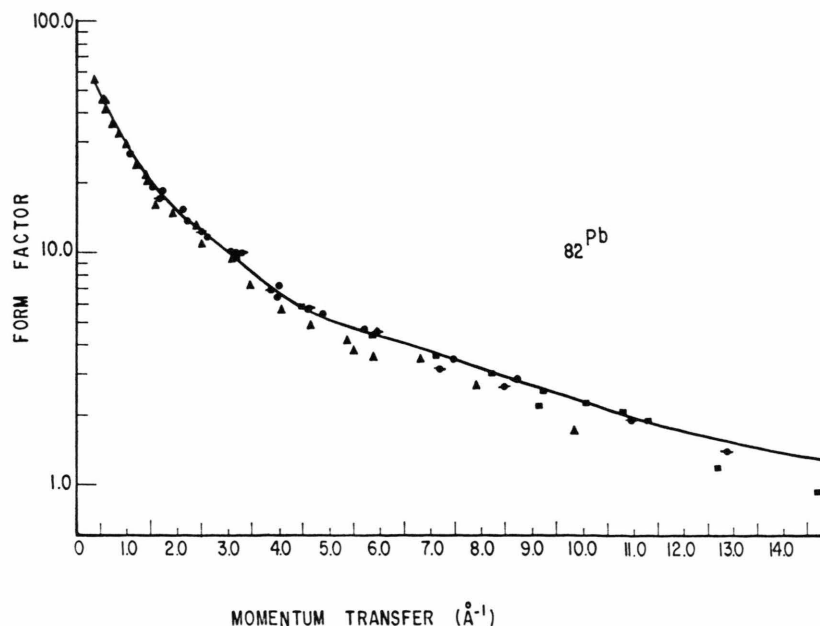


Fig. 3. Experimental form-factor of Pb compared with theoretical form-factor of Ref. [8]. ● present results; ■ Ref. [1]; ▲ Ref. [7].

In Fig. 3 the experimental form-factors for Pb from the present measurements are compared with previous results of Ref. [1], [6] and [7] and with (DHFS) form-factor results in the momentum transfer region $1-14 \text{ \AA}^{-1}$ [9]. Our results at 145 keV and 317 keV and the measurements of Schumacher [1] at 145 keV and 276 keV are in agreement with the calculated form-factor values. For momentum transfer $>6 \text{ \AA}^{-1}$ the form-factor theory fails, which was shown experimentally at 468 keV [6] and at 412 keV and 662 keV [1]. Deviations from the form-factor theory were found by other authors [7] for much smaller momentum

transfer, as can be seen in Fig. 3 and for energies above 244.7 keV. This shows that theories using the momentum transfer as only variable, cannot reproduce well all experiments.

Acknowledgements

The authors would like to thank the IEN Cyclotron staff, for their generous hospitality during measurements. This work was supported in part by Financiadora de Estudos e Projetos (FINEP) e Conselho Nacional de Desenvolvimento Científico e Tecnológico (CNPq).

- [1] F. Smend, M. Schumacher, and I. Borchert, Nucl. Phys. A **213**, 309 (1973); M. Schumacher, Phys. Rev. **182**, 7 (1969).
- [2] M. Schumacher and A. Stoffregen, Z. Physik A **283**, 15 (1977).
- [3] P. Rullhusen, F. Smend, and M. Schumacher, Z. Physik A **288**, 119 (1978).
- [4] S. K. Sen Gupta, N. C. Paul, S. C. Roy, and N. Lhandhuri, J. Phys. B **12**, 1211 (1979).
- [5] S. de Barros, O. Gonçalves, M. Gaspar, and J. R. Moreira, Phys. Rev. C **22**, 332 (1980).
- [6] S. de Barros, J. Eichler, O. Gonçalves, and M. Gaspar, to be published.
- [7] N. Ramanathan, T. J. Kenneth, and W. V. Prestwich, Can. J. Phys. **57**, 343 (1979).
- [8] J. H. Hubbel, J. Veigele Wm, E. A. Briggs, R. T. Brown, D. T. Cromer, and R. J. Howerton, J. Phys. Chem. Ref. Data, **4**, 471 (1975).
- [9] J. H. Hubbel and I. Overbø, J. Phys. Chem. Ref. Data, **8**, 69 (1979).
- [10] G. E. Brown and D. F. Mayers, Proc. Roy. Soc. A **234**, 387 (1955); G. E. Brown and D. F. Mayers, Proc. Roy. Soc. A **242**, 89 (1957).
- [11] D. T. Cromer and D. Liberman, J. Chem. Phys. **53**, 1891 (1970); Los Alamos, N. Mex., LA 4403 (1970).
- [12] W. R. Johnson and K. Cheng, Phys. Rev. A **13**, 692 (1976).
- [13] L. Kissel and R. H. Pratt, Report PITT-218 (1979).
- [14] L. Kissel and R. H. Pratt, Phys. Rev. Lett. **40**, 387 (1978).
- [15] S. Gopal and B. Sanjeevaiah, Nucl. Instrum. Meth. **107**, 221 (1973).
- [16] K. Siegbahn, Alpha-, Beta-, and gamma-ray Spectroscopy, North-Holland Pbl. Comp. 1968, p. 892 ff.
- [17] A. L. Conner, H. F. Atwater, E. H. Plassmann, and J. H. McCrary, Phys. Rev. A **1**, 539 (1970).
- [18] M. Gaspar, Thesis, Instituto de Física, Universidade Federal do Rio de Janeiro 1978 (Unpublished).